

Function of Extracellular Loop 2 in Rhodopsin: Glutamic Acid 181 Modulates Stability and Absorption Wavelength of Metarhodopsin II[†]

Elsa C. Y. Yan,^{‡,§} Manija A. Kazmi,^{§,||} Soma De,^{§,||} Belinda S. W. Chang,[§] Christoph Seibert,^{§,||} Ethan P. Marin,[§] Richard A. Mathies,[‡] and Thomas P. Sakmar^{*,§,||}

Department of Chemistry, University of California, Berkeley, California 94720, and Howard Hughes Medical Institute and Laboratory of Molecular Biology and Biochemistry, The Rockefeller University, New York, New York 10021

Received December 3, 2001; Revised Manuscript Received January 23, 2002

ABSTRACT: The second extracellular loop of rhodopsin folds back into the membrane-embedded domain of the receptor to form part of the binding pocket for the 11-*cis*-retinylidene chromophore. A carboxylic acid side chain from this loop, Glu181, points toward the center of the retinal polyene chain. We studied the role of Glu181 in bovine rhodopsin by characterizing a set of site-directed mutants. Sixteen of the 19 single-site mutants expressed and bound 11-*cis*-retinal to form pigments. The λ_{max} value of mutant pigment E181Q showed a significant spectral red shift to 508 nm only in the absence of NaCl. Other substitutions did not significantly affect the spectral features of the mutant pigments in the dark. Thus, Glu181 does not contribute significantly to spectral tuning of the ground state of rhodopsin. The most likely interpretation of these data is that Glu181 is protonated and uncharged in the dark state of rhodopsin. The Glu181 mutants displayed significantly increased reactivity toward hydroxylamine in the dark. The mutants formed metarhodopsin II-like photoproducts upon illumination but many of the photoproducts displayed shifted λ_{max} values. In addition, the metarhodopsin II-like photoproducts of the mutant pigments had significant alterations in their decay rates. The increased reactivity of the mutants to hydroxylamine supports the notion that the second extracellular loop prevents solvent access to the chromophore-binding pocket. In addition, Glu181 strongly affects the environment of the retinylidene Schiff base in the active metarhodopsin II photoproduct.

Rhodopsin (Rho)¹ is a prototypical member of the superfamily of G protein-coupled receptors (GPCRs) that serves as the dim light photoreceptor of the rod cell (1, 2). Following exposure to light, Rho assumes an active signaling conformation, metarhodopsin II (MII). MII can bind and catalytically activate the heterotrimeric G protein, transducin (G_t), to initiate the phototransduction cascade (3). The crystal structure of Rho provides a tool to elucidate important structure–activity relationships in Rho and in related GPCRs (4). These include, but are not limited to, the following: the structural basis of spectral tuning by visual pigments (5), the structural and physical basis for the ultrafast and specific photochemistry and high quantum efficiency of Rho (6, 7), the structural basis for the unusual stability of Rho in the

dark, and the molecular mechanism of receptor photoactivation (8). Here we focus on one unexpected and potentially important feature revealed in the crystal structure of Rho: the interaction between the second extracellular loop (E2) and the retinylidene (RET) chromophore and, in particular, the function of Glu181.

The extracellular surface domain of Rho comprises an amino-terminal tail and three extracellular interhelical loops: loop E1 (aa 101–106) connects transmembrane (TM) helix 2 and TM helix 3, loop E2 (aa 174–199) connects TM helix 4 and TM helix 5, and loop E3 (aa 278–285) connects TM helix 6 and TM helix 7. The E1 loop runs along the periphery of Rho. The E2 loop is folded deeply into the core of the membrane-embedded region of Rho in the proximity of the RET chromophore. E2 also forms extensive contacts with other extracellular regions. Gly174 and Met183 cross the membrane surface; the Met183 side chain points toward a hydrophobic pocket around TM helix 1, while the extended side chain of Gln184 is surrounded by relatively hydrophilic groups and a water molecule located close to the backbone carbonyl group of Pro180 and the hydroxyl group of Tyr192. The segment from Arg177 to Glu181 forms the β 3 strand, while that from Ser186 to Asp190 forms the β 4 strand.

One remarkable feature of the RET binding pocket in Rho is the presence of many polar or polarizable groups to coordinate an essentially hydrophobic ligand. The crystal structure of Rho reveals that at least 16 amino acid residues

[†] This research was supported in part by National Institutes of Health Training Grants GM07739, EY07138, GM07982, and EY02051 (to R.A.M.) and the Allene Reuss Memorial Trust (to T.P.S.). T.P.S. is an Associate Investigator of the Howard Hughes Medical Institute and a Senior Scholar of the Ellison Medical Foundation.

* To whom correspondence may be addressed at Box 284, Rockefeller University, 1230 York Ave., New York, New York 10021. Tel: 212-327-8288. Fax: 212-327-7904. E-mail: sakmar@mail.rockefeller.edu.

[‡] Department of Chemistry, University of California.

[§] Howard Hughes Medical Institute, The Rockefeller University.

^{||} Laboratory of Molecular Biology and Biochemistry, The Rockefeller University.

¹ Abbreviations: aa, amino acid; DM, *n*-dodecyl β -D-maltoside; E2, second extracellular loop of rhodopsin; GPCR, G protein-coupled receptor; G_t, transducin; MII, metarhodopsin II; RET, retinylidene chromophore of rhodopsin; Rho, rhodopsin; TM, transmembrane.

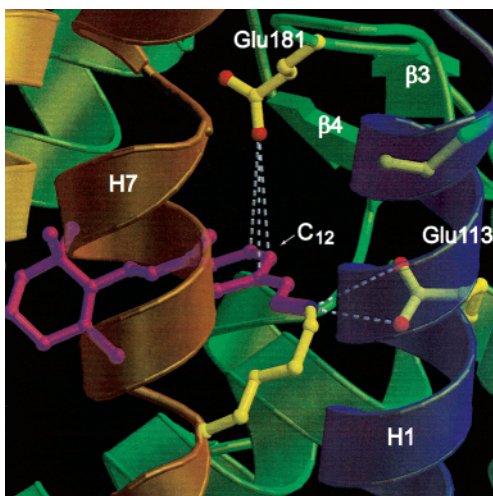


FIGURE 1: Molecular graphics diagram of the RET chromophore-binding pocket of Rho. The RET chromophore-binding pocket is shown within the plane of the membrane bilayer. TM helices are shown in ribbon format with helix 1 and helix 7 in the foreground. The $\beta 3$ and $\beta 4$ strands arise from E2. RET is colored magenta, and amino acid side chains are colored yellow except for nitrogen atoms (blue) and oxygen atoms (red). RET is situated such that its proximal end (approximately from C₉ to C₁₅) lies along the $\beta 4$ strand and its distal end (approximately from C₉ to the cyclohexenyl ring) lies along helix 3. One of the oxygen atoms of the side chain of Glu181 points toward C₁₂ of RET. This figure was prepared using Molscript (35) and Raster3D (33) and represents the A chain of the crystal structure coordinates (4).

are within 4.5 Å of the RET moiety: Glu113, Ala117, Thr118, Gly121, Glu122, Glu181, Ser186, Tyr191, Met207, His211, Phe212, Phe261, Trp265, Tyr268, Ala269, and Ala292. Three of these side chains, Glu181, Ser186, and Tyr191, are located on the E2 loop. In addition, Asp190 at the carboxyl-terminal end of the $\beta 4$ strand is interesting because although it is near the solvent-exposed surface of the receptor, its carboxyl group is partially buried. Asp190 appears to be coupled to the chromophore by its flanking residues Ile189 and Tyr191. Glu181, which arises at the carboxyl end of $\beta 3$ in the E2 loop, points toward the center of the polyene chain of RET (Figure 1).

Here we have carefully examined the role of Glu181 in Rho. We prepared and characterized a series of 19 single-site, and several double-site, mutants of bovine Rho with replacements of Glu181. Sixteen of the mutant pigments bound 11-*cis*-retinal to form pigments. Mutant pigment E181Q showed a significant spectral red shift only in the absence of NaCl. Other substitutions of Glu181 did not significantly affect the spectral features of the mutant pigments in the dark. The Glu181 mutants did display three significant phenotypes: (1) they generally had increased reactivity toward hydroxylamine, (2) they had shifted λ_{\max} values for their MII-like photointermediates, and (3) they had alterations in the decay rates of their MII-like photointermediates. There was no apparent correlation among these phenotypes and the amino acid side chain at position 181. These data suggest that Glu181 is protonated and uncharged in the dark state of Rho. Although Glu181 does not appear to contribute to spectral tuning of Rho, it does prevent solvent access to the Schiff base in the dark. On the basis of alterations in λ_{\max} values and stabilities of the MII-like photoproducts of the mutants, Glu181 more significantly affects the environment of the RET Schiff base in MII.

EXPERIMENTAL PROCEDURES

Preparation and Spectral Characterization of Rhodopsin Mutants. Site-directed point mutations were prepared using the QuikChange method (Stratagene) as described (9). Synthetic oligonucleotides were purchased from Genelink, Inc. DNA sequencing was carried out using BigDye Terminator Cycle sequencing in the DNA sequencing core facility at the Rockefeller University. Cell culture, transfection, and immunoaffinity purification procedures have been described elsewhere (10–12). Samples were generally obtained in 0.5 mM sodium phosphate buffer (pH 6.5) containing 0.1% (w/v) *n*-dodecyl β -D-maltoside (DM). UV-visible spectroscopy was carried out on a Perkin-Elmer Lambda 800 spectrophotometer set to a slit width of 2 nm in a cuvette with a path length of 1 cm. Samples were illuminated when indicated with a fiber-optic light (Fiber Lite A-200; Dolan Jenner Industries, Inc.) equipped with a >495 nm long-pass filter. All absorbance peak determinations were made on absolute spectra without subjecting the raw data to smoothing algorithms. In some cases, absorbance was plotted as a function of wavenumber (λ^{-1}), and the resulting curve was fit to a Gaussian function, which was used to determine the λ_{\max} value.

Measurement of Hydroxylamine Reactivity. The rates of reaction of mutant pigments with hydroxylamine were determined spectrophotometrically by monitoring the formation of retinal oxime ($\lambda_{\max} = 360$ nm) and the loss of absorbance at the visible λ_{\max} value of a particular pigment. Samples in 50 mM sodium phosphate buffer (pH 6.5) containing 0.1% (w/v) DM were kept in darkness at 25 °C. After a dark spectrum was recorded, reactions were started by adding buffered hydroxylamine solution to a final concentration of 50 mM, and samples were scanned at fixed time intervals using a slit width of 0.5 nm to minimize photobleaching from the probe beam. At the completion of each experiment, pH was checked, and a dark spectrum of a matched control sample kept in darkness was recorded. Data were fit to single-exponential functions to determine $t_{1/2}$ values. Each pigment was stable in darkness in the absence of hydroxylamine during the time course of the experiment.

Measurement of MII Decay by Fluorescence Spectroscopy. Fluorescence measurements of MII decay were carried out essentially as described (13) on a Spex Fluorolog 3-11 $\tau 3$ spectrofluorometer equipped with a 450 W xenon arc lamp. Fluorescence experiments were generally performed in 50 mM sodium phosphate buffer (pH 6.5) containing 0.1% (w/v) DM at 20 °C. Pigment concentrations were 80 nM in final sample volumes of 0.2 mL. For conversion to MII, samples were illuminated for 15 s using a fiber-optic light equipped with a >495 nm long-pass filter. Protein fluorescence traces were obtained by exciting at 295 nm and monitoring emission at 330 nm in 2 s pulses at 20–30 s intervals for 1.5–2 h. The excitation shutter was closed between acquisition pulses to minimize exposure to the measuring beam. The excitation and emission slit widths were 0.21 and 12 nm, respectively. Data were fit to single-exponential curves using the Origin software package. All fits showed r^2 values of >0.97 and the $t_{1/2}$ values reported in Table 1.

Table 1: Spectroscopic and Biochemical Characterization of Glu181 Mutants of Rho

sample	λ_{\max}^a (nm)		hydroxyl-amine reactivity ($t_{1/2}^b$ (min))	G_i activation rate ^c (%)	MII half-life ($t_{1/2}^d$ (min))
	dark	light			
Rho	501	382	5440 ± 170	100	12.5 ± 0.5 (3)
E181A	499	386	60.1 ± 4.0	82	17.3 ± 0.7 (3)
E181R ^e	nd ^h	nd	nd	nd	nd
E181N	500	384	25.1 ± 3.0	55	11 ± 1.0 (2)
E181D	497	383	1733 ± 357	94	7.7 ± 0.2 (3)
E181C	499	383	21.7 ± 2.0	nd	16.7 ± 0.5 (3)
E181Q	508/505 ^f	386	280 ± 9.0	76	5.2 ± 0.2 (3)
E181G	500	384	20.1 ± 4.3	59	6.5 ± 0.1 (3)
E181H	497	388	24.7 ± 5.0	66	10 ± 2.0 (4)
E181I	501	384	1.8 ± 0.2	46	9.0 (1) ^g
E181L	502	384	nd	nd	9.6 ± 0.9 (3)
E181K ^e	nd	nd	nd	nd	nd
E181M	500	383	5.0 ± 0.6	nd	15.4 ± 0.7 (3)
E181F	501	375	8.4 ± 0.4	77	52 ± 18 (5)
E181P ^e	nd	nd	nd	nd	nd
E181S	500	383	23.3 ± 1.7	nd	13.0 ± 0.1 (3)
E181T	502	383	6.0 ± 0.6	nd	17.3 ± 0.7 (3)
E181W	502	376	111 ± 4.0	80	27.5 ± 1.0 (3)
E181Y	501	392	9.8 ± 0.8	83	6.9 ± 0.1 (3)
E181V	498	383	5.7 ± 0.7	nd	12.0 ± 0.5 (3)
E113	499/385	nd	nd	nd	153 (1)
E113Q/E181D	500/387	nd	nd	nd	nd
E113Q/E181H ^e	nd	nd	nd	nd	nd
E113Q/E181Q ^e	nd	nd	nd	nd	nd
E113Q/E181F ^e	nd	nd	nd	nd	nd
E113Q/E181W ^e	nd	nd	nd	nd	nd

^a Values for λ_{\max} were determined from absolute spectra using either the instrument peak finding algorithm or fitting the data to a Gaussian function as described in Experimental Procedures. All λ_{\max} values are estimated to be precise to ±1 nm. ^b Rates of reaction with hydroxyl-amine were calculated from best-fit exponentials of absorbance as a function of time of the visible-absorbing pigment peak. Values are presented as $t_{1/2} \pm r$, where r represents the error of the curve fit. Values calculated using the absorbance of the retinal oxime peak were nearly identical to those determined using the visible-absorbing peak. ^c Activation rates were normalized to that of Rho assayed under identical conditions. Values reported are the average of two independent determinations. Rates were determined for only a subset of mutant pigments in order to interpret the results of the MII decay experiments. Constitutive activity was not detected in detergent solution for any of the mutants assayed. ^d MII decay rates were calculated from best-fit exponentials. Values are presented as the mean $t_{1/2} \pm \text{SEM}$ (n), where n represents the number of independent experiments. ^e Mutant did not bind 11-*cis*-retinal to form a stable pigment. ^f Values for λ_{\max} of mutant E181Q were determined in the absence (508 nm) or presence (505 nm) of 200 mM NaCl. ^g Mutant E181I showed some increase in fluorescence before photolysis consistent with thermal instability. ^h nd = not determined.

Fluorescence G_i Activation Assay. G_i was prepared from frozen bovine retinas (Lawson, Inc., Lincoln, NE) using standard techniques (14, 15) modified as reported (16). The assay was performed essentially as described using 250 nM G_i and 2 nM Rho or mutant pigment (17).

RESULTS

Preparation and UV-Visible Spectroscopy of Site-Directed Mutants. Nineteen single-replacement mutants of Rho were prepared in which the glutamic acid at position 181 was replaced by each of the other 19 amino acids. In addition, five double-replacement mutants were prepared in which E113Q was combined with one of the Glu181 mutants (E181D, E181F, E181Q, E181H, or E181W). The mutants were transiently expressed in COS cells and regenerated with

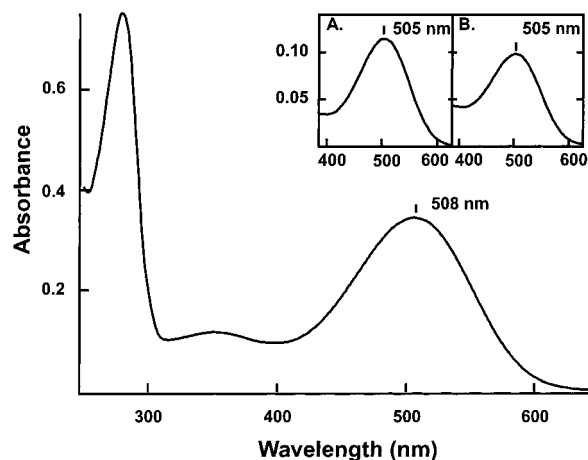


FIGURE 2: Visible absorbance spectroscopy of mutant pigment E181Q. A UV-visible absorbance spectrum was recorded for purified mutant pigment E181Q in the absence of NaCl at pH 6.5. The λ_{\max} values are indicated for each spectrum. The λ_{\max} values for the entire set of Glu181 mutants are listed in Table 1. Inset: (A) Visible spectrum of E181Q at pH 6.5 after the addition of NaCl to a final concentration of 200 mM. (B) Visible spectrum of E181Q in 200 mM NaCl at pH 4.5.

11-*cis*-retinal. The mutant pigments were purified by an established immunoaffinity adsorption procedure in DM detergent buffer. UV-visible spectra were recorded on purified samples in the dark. In general, the level of opsin expression was reduced for each mutant on the basis of the absorbance at 280 nm of the purified sample. Most mutants expressed to about 30–50% of the level of Rho. Only mutants E181D, E181Q, and E181M expressed reproducibly to levels above 50% of that of Rho. Mutants E181R, E181K, and E181P expressed to <20% of the level of Rho. These three mutants (E181R, E181K, and E181P) also failed to yield a stable pigment when incubated with 11-*cis*-retinal as judged by the lack of a visible-absorbing spectral peak after purification.

The λ_{\max} values of the dark forms of the mutant Glu181 pigments are presented in Table 1. Under conditions where Rho displayed a λ_{\max} value of 501 nm, the λ_{\max} values of the mutant pigments, excluding E181Q, ranged from 497 nm for E181D and E181H to 502 nm for E181L, E181T, and E181W. Although the mutations caused minor reproducible spectral alterations, the salient result is that mutation of Glu181 did not significantly shift the λ_{\max} values of the resulting mutant pigments. Only mutant pigment E181Q showed a significant bathochromic spectral shift (λ_{\max} value of 508 nm) compared with the other mutants under the conditions of low salt studied (0.5 mM sodium phosphate with no added NaCl) (Figure 2). Extensive dialysis of the E181Q sample against a solution of 0.5 mM sodium phosphate and 0.1% (w/v) DM to remove any salt retained after the immunoaffinity adsorption procedure did not result in a further reproducible spectral shift of E181Q. In addition, the dialysis experiment suggested that the λ_{\max} value of 508 nm is consistent with a pigment that is free of bound anions other than the possibility of phosphate, which is present in the buffer at 0.5 mM. Addition of NaCl to the E181Q pigment prepared in the absence of chloride anions caused a modest shift in λ_{\max} value to 505 nm (Figure 2, Table 1). These spectral features of E181Q were similar to results reported previously, although we did not observe a NaCl-

dependent shift to a wild-type λ_{\max} value of 501 nm (18, 19). No significant NaCl effect on λ_{\max} value was noted for any of the other Glu181 mutant pigments.

The dark spectrum of mutant E181Q was also tested for anion dependency and pH dependency (18, 20). There were slight differences in λ_{\max} values in the presence of formate (511 nm), fluoride (506 nm), and acetate (508 nm) at concentrations of 100–500 mM (not shown). Each of these values fell close to the range of λ_{\max} values obtained from different preparations of E181Q in the presence of 200 mM chloride (505–508 nm). No pH dependency was noted in the λ_{\max} value of E181Q in the presence of 4 mM or 200 nM NaCl over the pH range of 4.5 to about 8 (Figure 2).

Double-replacement mutants were prepared in which mutant E113Q was combined with various Glu181 mutants (Table 1). All of the five double-replacement mutant opsins expressed poorly, and four of the five mutants failed to bind 11-*cis*-retinal to form stable pigments (E113Q/E181H, E113Q/E181Q, E113Q/E181F, and E113Q/E181W). Only mutant E113Q/E181D bound retinal to form a stable pigment, albeit at low levels (about 5-fold less than E113Q expressed and purified in parallel). Like mutant E113Q, the E113Q/E181D mutant pigment displayed a pH-dependent equilibrium in the dark between UV- and visible-absorbing spectral forms. The acidity constant (pK_a) of the transition between the two spectral forms was 6, which was identical to that measured for E113Q and also reported earlier (10).

Photolysis of Purified Recombinant Pigments and Spectral Characterization of MII-like Photoproducts. Each of the Glu181 mutant pigments was photoactive. For example, in the case of mutant pigment E181Q, illumination with light of $\lambda > 495$ nm produced a gradual decrease in the visible-absorbing peak with a concomitant increase in a UV-absorbing peak. The appearance of the UV-absorbing peak was consistent with the formation of a MII-like photoproduct. An isosbestic point was noted for the transition between the two spectral forms, which is consistent with the conversion of the dark state of the pigment to a MII-like form without a significant accumulation of a metarhodopsin I-like form that might be expected to absorb in the visible region. The same behavior is observed in the case of Rho in DM solution where photolysis converts the pigment rapidly to MII. Photobleaching difference spectra of representative mutant pigments are presented in Figure 3. The shapes of the curves suggest a complete transition to a MII-like form upon photolysis in each case.

The λ_{\max} values of the UV-absorbing forms of the mutant Glu181 pigments that formed immediately after photolysis are presented in Table 1. There were significant differences in the λ_{\max} values of the MII-like spectral forms among the Glu181 mutants. Absolute spectra of selected mutants are presented in Figure 4 where absorbance is plotted as a function of wavelength. Each of the MII-like spectra was recorded under conditions where the RET Schiff base was intact as judged by the formation of a 440 nm peak upon acid denaturation. Under conditions where the MII form of Rho displayed a λ_{\max} value of 382 nm, the λ_{\max} values of the MII-like forms of the Glu181 pigments varied from 375 to 392 nm for E181F and E181Y, respectively.

Hydroxylamine Reactivity of Purified Recombinant Pigments. Hydroxylamine has been used extensively as a chemical probe of the accessibility of the Schiff base linkage

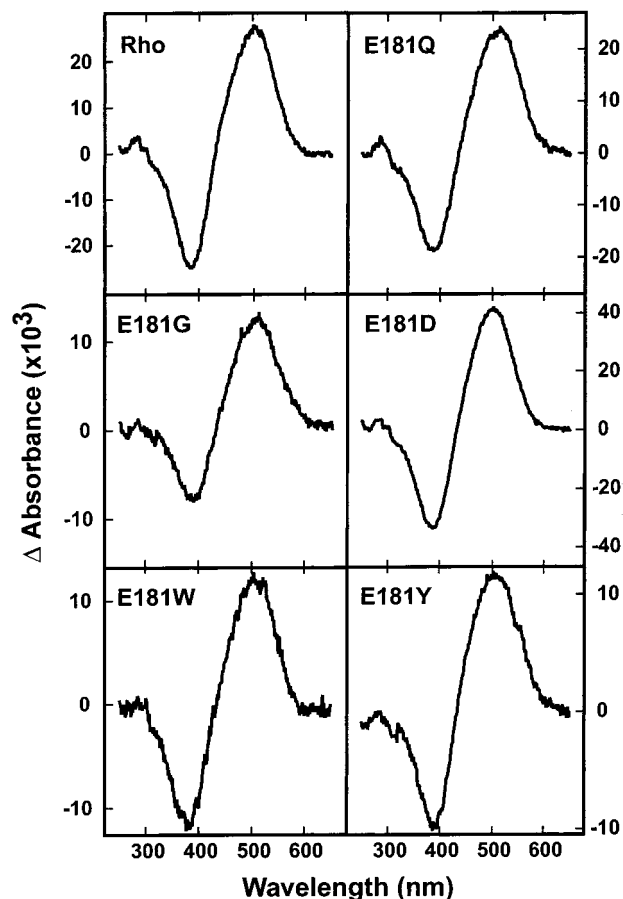


FIGURE 3: Photobleaching difference spectra of expressed Rho and selected mutant pigments. For each pigment (Rho, E181Q, E181G, E181D, E181W, and E181Y), a dark spectrum and a spectrum after illumination were recorded. The calculated difference spectrum is presented where the change in absorbance (dark minus light) is plotted as a function of wavelength. Spectra are presented without alteration of data by averaging or smoothing algorithms. Values for λ_{\max} determined from absolute spectra are presented in Table 1.

in Rho and in mutant Rhos. The rate of hydroxylamine reactivity was determined for each of the Glu181 mutants in darkness (Table 1). Rho does not react significantly with hydroxylamine in the dark under the conditions assayed ($t_{1/2} = 5440$ min). Each of the Glu181 mutants was more reactive to hydroxylamine than Rho assayed under identical conditions. Several of the Glu181 mutants (E181F, E181T, and E181Y) displayed reaction rates that were greater than 500-fold increased over that of Rho. Mutant E181Q reacted with hydroxylamine with a reaction rate that was nearly 20-fold greater than that of Rho.

MII Decay Rates and G_i Activation Rates of Solubilized Purified Recombinant Pigments. The rates of decay of the MII-like photoproducts of the Glu181 mutant pigments were measured in a kinetic fluorescence assay (13). The decay of MII was observed as an increase in the intrinsic tryptophan fluorescence of Rho upon release of the all-*trans*-retinal from its binding pocket, which reduces fluorescence quenching. It was previously reported that the rate of fluorescence increase in this assay is very similar to the rate of decay of R^* , the active state of Rho that catalyzes GTP γ S uptake by G_i . The rate of fluorescence increase is thought also to reflect the rate of Schiff base hydrolysis in the MII photoproduct of Rho. Under the conditions of the assay, the half-life of

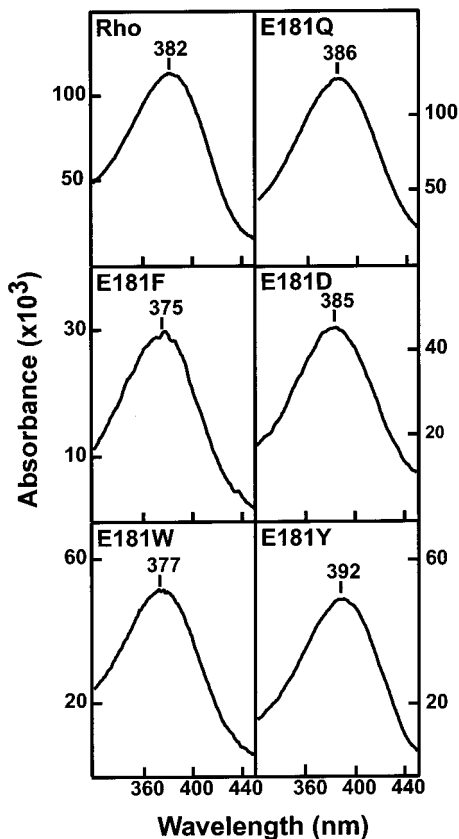


FIGURE 4: UV absorbance spectroscopy of expressed Rho and selected mutant pigments. For each pigment (Rho, E181Q, E181F, E181D, E181W, and E181Y), a spectrum was recorded after illumination. Absorbance was plotted as a function of wavelength in the range of the MII-like photoproduct peak. Values for λ_{\max} determined from curve fits are indicated in the figure and are listed in Table 1 for the entire set of mutants.

MII decay was 12.5 min, which confirmed results reported earlier (13). As a control, the half-life of decay of the MII-like photoproduct of mutant pigment E113Q was also measured. The MII-like form of E113Q was previously reported to have a slow rate of Schiff base hydrolysis as measured by serial acid denaturation (10). The half-life measured in the fluorescence assay ($t_{1/2} = 153$ min) was similar to that reported earlier.

The half-life of decay was measured for the MII-like photoproduct of each of the Glu181 mutant pigments (Figure 5 and Table 1). The decay half-life values varied significantly among the Glu181 mutants and ranged from 6.5 min for mutant E181G to 52 min for E181F. The MII-like photoproducts of mutants E181D, E181Q, E181G, E181I, E181L, and E181Y decayed significantly more rapidly than MII. The photoproducts of E181A, E181C, E181M, E181F, E181T, and E181W decayed significantly more slowly than MII. The decay half-life values of the photoproducts of E181N, E181H, E181S, and E181V were the same as that of MII. The decay half-life values of MII and the MII-like photoproduct of E181Q were not significantly affected by varying NaCl concentrations from 0 to 300 mM (not shown).

The rates of GTP γ S uptake by G_t catalyzed by photoactivated Glu181 mutants were measured using an established fluorescence assay under conditions where the pigment concentration should be rate limiting (17). Fluorescence traces are presented for selected mutant pigments in Figure

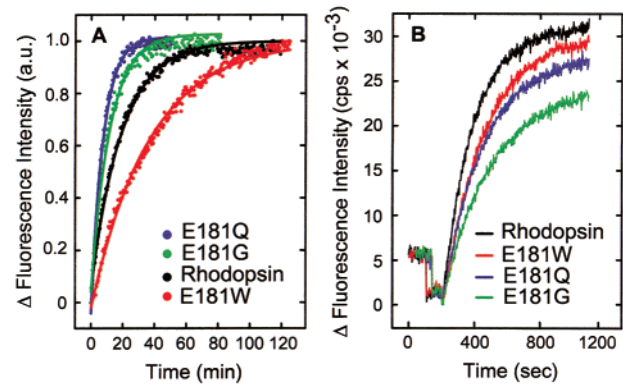


FIGURE 5: Measurements of MII decay rates and G_t activation rates of expressed Rho and mutant pigments E181Q, E181G, and E181W. (A) Decay of MII was monitored as the increase in tryptophan fluorescence intensity as a function of time. Purified Rho or a Glu181 replacement mutant (80 nM) was incubated at 20 °C for 10 min and then bleached for 15 s to photoconvert the pigment to MII. Fluorescence was recorded immediately following photolysis. Normalized data points are plotted and fit to single-exponential curves. A complete data set of calculated $t_{1/2}$ values is presented in Table 1. (B) The rate of G_t activation that was catalyzed by Rho or a Glu181 replacement mutant was monitored at 10 °C as the increase in intrinsic fluorescence intensity of G_t following uptake of GTP γ S. Purified Rho or a Glu181 replacement mutant (2 nM) was added at 100–150 s to a cuvette containing bovine G_t (250 nM) under continuous illumination. The reaction was initiated at 200 s by the addition of GTP γ S (5 mM). The fluorescence intensity immediately following GTP γ S addition was normalized to zero. The rates of G_t activation were determined by linear regression through the first 30–60 s of data after the addition of GTP γ S. A complete data set of G_t activation for the selected mutant pigment relative to that of Rho is presented in Table 1.

5. Values normalized to the value for Rho assayed in parallel are presented in Table 1. Each of the mutants tested was able to activate G_t. In general, the mutant pigments displayed slight to moderate defects in the ability to activate G_t.

To understand the defects in G_t activation caused by mutation of Glu181, one needs to consider two factors. First, the decay of the MII-like photoproduct could lead to a decrease in G_t activation rate. This effect will not be observable if the decay of the MII-like photoproduct is much slower than the rate of G_t activation. Second, defects in the structures of MII-like photoproducts can lead to changes in their G_t activation rates. For example, substitution of Glu181 might change the effectiveness of the resulting MII-like photoproduct in coupling to G_t and in turnover efficiency. When the entire set of mutants is considered, there does not appear to be a significant correlation between the rate of MII-like photoproduct decay and the rate of G_t activation. This result is not surprising because the observed rate of G_t activation is coupled not only to the rate of MII-like photoproduct decay but also to G_t association rate and turnover rate. Mutation of Glu181 can exert additive or canceling effects on the kinetics of G_t activation through these processes.

DISCUSSION

In Rho, Glu181, which arises from the linker between β 3 and β 4 in the E2 loop and points toward the center of the polyene chain of RET, is particularly interesting (Figure 1). The potential for an ionic interaction between Glu181 and RET suggests that it may have a role in the mechanism of

the opsin shift. Perturbation of the electron distribution near the center of the polyene chain is one mechanism to facilitate spectral tuning according to the "point-charge model" of the opsin shift (21). Glu113, the RET Schiff base counterion, was predicted to be located near C₁₂ of the RET polyene by two-photon spectroscopy and NMR spectroscopy of retinal analogues and semiempirical quantum mechanical orbital calculations (22, 23). Although the crystal structure confirmed that Glu113 is near the Schiff base nitrogen, it is not simultaneously near C₁₂ of RET. In fact, Glu181 is situated so that one of its carboxylic acid oxygen atoms is approximately 4.2 Å from the C₁₂ of RET. The crystal structure resolution is not high enough to determine the protonation states of carboxylic acid side chains (4).

Glu181 is highly conserved among vertebrate opsins and blue and UV cone pigments. All visual pigments appear to contain either a glutamic acid or an aspartic acid at position 181, with the notable exceptions of the long-wavelength cone pigments and the salmon VA opsin (19). The corresponding position in human green and red cone pigments is His197, which forms part of a chloride ion binding site. Chloride binding causes a red shift in absorption of the green and red pigments. Interestingly, the H197E/R200Q mutant of the human green cone pigment displays a visible λ_{\max} value of 500 nm (24), which is the same as the λ_{\max} value of Rho, suggesting that perturbation of the polyene by chloride may be the only element in the green cone pigment responsible for its spectral difference from Rho. It seems plausible that a chloride ion held in place by His197 and Lys200 might interact with the central portion of the polyene of RET in these pigments. The negative charge of the chloride ion bound to His197 in the long-wavelength sensing cone pigments might be brought closer to RET than the charge of a potential carboxylate of Glu181 in Rho (25).

Retinochrome is a remote relative of Rho that functions as a retinal photoisomerase that converts all-*trans*-retinal to 11-*cis* after light absorption. Like Rho, the retinylidene chromophore of retinochrome forms a protonated Schiff base linkage with a conserved lysine residue on TM helix 7. Like invertebrate visual pigments, retinochrome lacks a carboxylic acid residue at position 113. Instead, a conserved glutamic acid residue at position 181 was reported to serve as the counterion as judged by spectral analysis of site-directed mutants (19). The spectral phenotype of retinochrome mutant E181Q was similar to that of Rho mutant E113Q. In the same study, Rho mutant E181Q was reported to show a normal spectrum that became red shifted to 510 nm in the absence of chloride. It was concluded that Glu181 in bovine Rho did not serve a counterion function but that it did affect spectral absorption characteristics.

All vertebrate Rhos contain either a glutamic acid or an aspartic acid at position 113. Invertebrate pigments do not (10, 19). Glu113 was identified to be the retinylidene Schiff base counterion on the basis of specific results from a number of experimental approaches (10, 18, 20, 26). Replacement of Glu113 by glutamine caused a dramatic decrease in the pK_a of the Schiff base from >12 in Rho (27) to about 6 in mutant E113Q. The mutant pigment E113Q displayed a pH-dependent equilibrium between protonated and unprotonated Schiff base forms. Schiff base protonation was dependent on the presence of solute anions, and the λ_{\max} value varied depending on the anion present. Resonance Raman spec-

troscopy of the acidic form of E113Q showed that the protonated C=NH vibrational mode was shifted (28). An FTIR spectroscopic analysis identified a specific difference band that was assigned to the protonation of Glu113 upon MII formation (29, 30). Glu113 was also demonstrated to be the proton acceptor in the Schiff base deprotonation reaction (30). Finally, the mutant E113D displayed a red-shifted λ_{\max} value and a slow transition from metarhodopsin I to MII, consistent with an increase in the distance between Schiff base and its counterion (10, 26).

Does Glu181 serve as a second counterion or contribute to charge neutralization of the protonated Schiff base? Replacement of Glu181 by glutamine resulted in a mutant pigment that bound 11-*cis*-retinal to give a pigment that displayed a λ_{\max} value of 505 nm. The E181Q pigment did not display a blue-shifted λ_{\max} value. The λ_{\max} value of E181Q was dependent on the concentration of NaCl in the solution, but the chloride-dependent spectral shift was very small (λ_{\max} of 508 nm in the absence of salt). There was no significant dependency of λ_{\max} value on the nature of the anion for several anions tested. In addition, there was no pH dependency in the λ_{\max} value of the dark form of E181Q. The other Glu181 replacement mutants displayed dark spectra with only very slight spectral shifts from wild type. These results show that Glu181 does not contribute significantly to spectral tuning of the λ_{\max} value and suggest that Glu181 is protonated and uncharged in the ground state of Rho.

Double-replacement mutants were prepared to test the hypothesis that the Schiff base pK_a of Glu113 mutants should be sensitive to the amino acid side chain at position 181 if it is in the vicinity of the Schiff base. Interestingly, only one of the double-replacement mutants tested was able to bind 11-*cis*-retinal to yield a stable pigment. One interpretation of this negative result would be that Glu181 serves at least as a partial Schiff base counterion in the absence of Glu113, even though a solute anion is still required to observe the visible-absorbing form of E113Q. However, since these four double-replacement mutants expressed at very low levels, the more reasonable explanation in the context of the entire data set is that these mutant opsins were not properly folded and failed to reach a mature structure in the plasma membrane. This phenotype has been commonly reported for opsins with mutations in the extracellular loops of Rho (31). Mutant E113Q/E181D did form a stable pigment in the dark, albeit at low yield. It behaved in general like mutant E113Q. However, although E113Q/E181D showed a pH-dependent equilibrium between two spectral forms, there was no difference in the Schiff base pK_a value of the double mutant compared with that of the single mutant E113Q. The apparent Schiff base pK_a values of both mutants were 6.

Hydroxylamine is a useful chemical probe of Schiff base accessibility and reactivity. Only the replacement to aspartic acid in mutant E181D preserved the resistance of Schiff base reactivity (approximately 3-fold increased reactivity). Other replacements caused dramatic increases in hydroxylamine reactivity even when the pigment was stable in darkness in solution for extended times at 25 °C. Only mutants E181I and E181V showed detectable thermal instability in the dark over 24–48 h. The crystal structure of Rho shows that E2 folds in toward the chromophore. The increased hydroxylamine reactivity of the Glu181 mutants confirms that the

E2 loop prevents solvent access to the RET Schiff base in the dark.

All of the mutants, including E181Q, showed normal bleaching kinetics to a MII-like spectral form under the conditions tested. However, although the Glu181 replacement mutants displayed dark spectra with only slight spectral shifts, the λ_{\max} values of several of the MII-like photoproducts of the Glu181 mutants were shifted. The values ranged from 375 nm for E181F to 392 nm for E181Y under conditions where the λ_{\max} value of MII was 382. The energy difference between λ_{\max} values of 375 and 392 nm is 1157 wavenumbers (cm^{-1}). The same energy difference would represent a visible λ_{\max} range of 484–513 nm if applied to an index λ_{\max} value of 500 nm rather than 382 nm. Therefore, the interaction between Glu181 and RET appears to be more pronounced in the active MII-like photoproduct than in the ground state.

The rates of decay of the MII-like photoproducts of the Glu181 mutants were measured. The assay directly measures the increase in intrinsic tryptophan fluorescence as all-*trans*-retinal leaves its binding pocket. Loss of all-*trans*-retinal must involve at least a two-step process: Schiff base hydrolysis followed by diffusion of the chromophore from its binding pocket. Chromophore diffusion may be rate limiting, but it obviously must occur after Schiff base hydrolysis in an otherwise properly folded pigment. It was suggested earlier that Glu113 was involved in the autocatalytic hydrolysis of the Schiff base linkage of MII (10). Interestingly, whereas the mutant E113Q was noted to have a low rate of Schiff base decay, the decay rate of the MII-like photoproduct of E181Q was significantly increased. Two mutants (E181F and E181W) displayed significantly decreased rates of decay of the MII-like photoproduct. However, neither rate approached that of mutant E113Q (153 min), suggesting that Glu113 was still involved in the Schiff base hydrolysis reaction in these Glu181 mutants. Glu181 seems to be involved in controlling the rate of Schiff base hydrolysis after photolysis. It cannot be ruled out at present that mutations with decreased decay rates caused an enhanced binding of the all-*trans*-retinal after Schiff base hydrolysis. However, preliminary measurements of decay rates as a function of temperature suggest that Schiff base hydrolysis may be rate limiting in all of the mutants tested. The mechanism by which mutation of Glu181 might modulate the rate of Schiff base hydrolysis in the single replacement mutants is under investigation.

In summary, the Glu181 mutants displayed three interesting phenotypes: (1) they generally had increased reactivity toward hydroxylamine, (2) they had shifted λ_{\max} values for their MII-like photointermediates, and (3) they had alterations in the decay rates of their MII-like photointermediates. There was no apparent correlation among these phenotypes and the amino acid side chain at position 181. For example, mutants with the highest rates of MII-like photoproduct decay did not all have red-shifted λ_{\max} values for their MII-like photoproducts. Perhaps even more striking than the phenotypes outlined above is the lack of significant effects of mutation of Glu181 on the spectral features of the mutant pigments in the dark. The most likely interpretation of the data at hand is that Glu181 is protonated and uncharged. Data from Glu181 mutants provide no significant indication that Glu181 is charged in the dark state of Rho or that it contributes significantly to spectral tuning. However, the data

do not exclude the possibility that Glu181 might mediate association, either directly or indirectly, with a loosely bound solute anion. Such an anion was not appreciated in the crystal structure of Rho.

What is the functional role of Glu181 in Rho? The evidence presented here shows that Glu181 affects the environment of the RET Schiff base primarily in MII but also in the dark, at least as judged by hydroxylamine reactivity experiments. However, we cannot rule out an influence of Glu181 on other photoproducts. Glu181 may be influencing the photochemistry of Rho, the kinetics of formation of early photoproducts, or the precise chromophoric structures of the photoproducts. For example, Glu181 may serve to influence the electron density of the conjugated polyene system of the RET chromophore so that photoisomerization occurs exclusively at the C₁₁–C₁₂ double bond. Preresonance Raman and time-resolved UV–visible spectroscopy experiments are in progress to address these possible roles of Glu181.

ACKNOWLEDGMENT

We thank Dr. A. Gopala Krishna, Dr. Santosh Menon, Dr. May Han, Anthony Sanfiz, and Karolina Jönsson for assistance with these experiments or for their interpretation.

REFERENCES

- Menon, S. T., Han, M., and Sakmar, T. P. (2001) *Physiol. Rev.* 81, 1659–1688.
- Ballesteros, J. A., Shi, L., and Javitch, J. A. (2001) *Mol. Pharmacol.* 60, 1–19.
- Stryer, L. (1991) *J. Biol. Chem.* 266, 10711–10714.
- Palczewski, K., Kumasaka, T., Hori, T., Behnke, C. A., Motoshima, H., Fox, B. A., Le Trong, I., Teller, D. C., Okada, T., Stenkamp, R. E., Yamamoto, M., and Miyano, M. (2000) *Science* 289, 739–745.
- Kochendoerfer, G. G., Lin, S. W., Sakmar, T. P., and Mathies, R. A. (1999) *Trends Biochem. Sci.* 24, 300–305.
- Wang, Q., Schoenlein, R. W., Peteanu, L. A., Mathies, R. A., and Shank, C. V. (1994) *Science* 266, 422–424.
- Mathies, R. A., and Lugenburg, J. (2000) in *Molecular Mechanisms in Visual Transduction* (Stavenga, D. G., de Grip, W. J., and Pugh, E. N., Jr., Eds.) pp 55–90, Elsevier Science, New York.
- Sakmar, T. P. (1998) *Prog. Nucleic Acid Res. Mol. Biol.* 59, 1–34.
- Marin, E. P., Gopala Krishna, A., Archambault, V., Simuni, E., Fu, W.-Y., and Sakmar, T. P. (2001) *J. Biol. Chem.* 276, 23873–23880.
- Sakmar, T. P., Franke, R. R., and Khorana, H. G. (1989) *Proc. Natl. Acad. Sci. U.S.A.* 86, 8309–8313.
- Min, K. C., Zvyaga, T. A., Cypess, A. M., and Sakmar, T. P. (1993) *J. Biol. Chem.* 268, 9400–9404.
- Han, M., Lin, S. W., Minkova, M., Smith, S. O., and Sakmar, T. P. (1996) *J. Biol. Chem.* 271, 32337–32342.
- Farrens, D. L., and Khorana, H. G. (1995) *J. Biol. Chem.* 270, 5073–5076.
- Kuhn, H. (1980) *Nature* 283, 587–589.
- Fung, B. K., Hurley, J. B., and Stryer, L. (1981) *Proc. Natl. Acad. Sci. U.S.A.* 78, 152–156.
- Min, K. C., Gravina, S. A., and Sakmar, T. P. (2000) *Protein Expression Purif.* 20, 514–526.
- Fahmy, K., and Sakmar, T. P. (1993) *Biochemistry* 32, 7229–7236.
- Nathans, J. (1990) *Biochemistry* 29, 9746–9752.
- Terakita, A., Yamashita, T., and Shichida, Y. (2000) *Proc. Natl. Acad. Sci. U.S.A.* 97, 14263–14267.
- Sakmar, T. P., Franke, R. R., and Khorana, H. G. (1991) *Proc. Natl. Acad. Sci. U.S.A.* 88, 3079–3083.

21. Honig, B., Dinur, U., Nakanishi, K., Balogh-Nair, V., Gawinowicz, M. A., Arnaboldi, M., and Motto, M. (1979) *J. Am. Chem. Soc.* *101*, 7084–7086.
22. Birge, R. R. (1990) *Biochim. Biophys. Acta* *1016*, 293–327.
23. Han, M., DeDecker, B. S., and Smith, S. O. (1993) *Biophys. J.* *65*, 899–906.
24. Wang, Z., Asenjo, A. B., and Oprian, D. D. (1993) *Biochemistry* *32*, 2125–2130.
25. Kochendoerfer, G. G., Wang, Z., Oprian, D. D., and Mathies, R. A. (1997) *Biochemistry* *36*, 6577–6587.
26. Zhukovsky, E. A., and Oprian, D. D. (1989) *Science* *246*, 928–930.
27. Steinberg, G., Ottolenghi, M., and Sheves, M. (1993) *Biophys. J.* *64*, 1499–1502.
28. Lin, S. W., Sakmar, T. P., Franke, R. R., Khorana, H. G., and Mathies, R. A. (1992) *Biochemistry* *31*, 5105–5111.
29. Fahmy, K., Jager, F., Beck, M., Zvyaga, T. A., Sakmar, T. P., and Siebert F. (1993) *Proc. Natl. Acad. Sci. U.S.A.* *90*, 10206–10210.
30. Jager, F., Fahmy, K., Sakmar, T. P., and Siebert, F. (1994) *Biochemistry* *33*, 10878–10882.
31. Doi, T., Molday, R. S., and Khorana, H. G. (1990) *Proc. Natl. Acad. Sci. U.S.A.* *87*, 4991–4995.
32. Kraulis, P. J. (1991) *J. Appl. Crystallogr.* *24*, 946–950.
33. Merritt, E. A., and Bacon, D. J. (1997) *Methods Enzymol.* *277*, 505–524.

BI0160011